

Review of thermal transport and electronic properties of borophene

Dengfeng Li(李登峰), Ying Chen(陈颖), Jia He(何佳), Qiqi Tang(汤琪琪), Chengyong Zhong(钟承勇), Guangqian Ding(丁光前)
Citation: Chin. Phys. B . 2018, 27(3): 036303. **doi:** 10.1088/1674-1056/27/3/036303

Journal homepage: http://cpb.iphy.ac.cn; http://iopscience.iop.org/cpb

What follows is a list of articles you may be interested in

Two-dimensional thermal illusion device with arbitrary shape based on complementary media

Ge Xia(夏舸), Wei Kou(寇蔚), Li Yang(杨立), Yong-Cheng Du(杜永成)
Chin. Phys. B . 2017, 26(10): 104403. **doi:** 10.1088/1674-1056/26/10/104403

Thermal properties of two-dimensional materials

Gang Zhang(张刚), Yong-Wei Zhang(张永伟)
Chin. Phys. B . 2017, 26(3): 034401. **doi:** 10.1088/1674-1056/26/3/034401

A technique for simultaneously improving the product of cutoff frequency-breakdown voltage and thermal stability of SOI SiGe HBT

Qiang Fu(付强), Wan-Rong Zhang(张万荣), Dong-Yue Jin(金冬月), Yan-Xiao Zhao(赵彦晓), Xiao Wang(王肖)
Chin. Phys. B . 2016, 25(12): 124401. **doi:** 10.1088/1674-1056/25/12/124401

Time fractional dual-phase-lag heat conduction equation

Xu Huan-Ying, Jiang Xiao-Yun
Chin. Phys. B . 2015, 24(3): 034401. **doi:** 10.1088/1674-1056/24/3/034401

Reversal of thermal rectification in one-dimensional nonlinear composite system

Zhan Si-Qi, Huang Wei-Qing, Huang Gui-Fang
Chin. Phys. B . 2014, 23(11): 114401. **doi:** 10.1088/1674-1056/23/11/114401

TOPIC REVIEW — Thermal and thermoelectric properties of nano materials

Review of thermal transport and electronic properties of borophene

Dengfeng Li(李登峰)†, Ying Chen(陈颖), Jia He(何佳), Qiqi Tang(汤琪琪), Chengyong Zhong(钟承勇), and Guangqian Ding(丁光前)

School of Science, Chongqing University of Posts and Telecommunications, Chongqing 400065, *China*

(Received 20 October 2017; revised manuscript received 29 December 2017; published online 11 February 2018)

In recent years, two-dimensional boron sheets (borophene) have been experimentally synthesized and theoretically proposed as a promising conductor or transistor with novel thermal and electronic properties. We first give a general survey of some notable electronic properties of borophene, including the superconductivity and topological characters. We then mainly review the basic approaches, thermal transport, as well as the mechanical properties of borophene with different configurations. This review gives a general understanding of some of the crucial thermal transport and electronic properties of borophene, and also calls for further experimental investigations and applications on certain scientific community.

Keywords: borophene, thermal transport, electronic property

PACS: 44.10.+i, 65.80.–g, 63.22.–m **DOI:** 10.1088/1674-1056/27/3/036303

1. Introduction

The fundamental physical properties of materials, such as thermal and electronic properties, are crucial to the performance and longevity of nano-devices. With the miniaturization of electronic devices, such as transistors, the silicon-based devices are not well suitable for the high standard of electronic transport and thermal diffusion in nano-devices. The discovery of graphene brings some light to this field for its ultra-fast electronic transport properties and high thermal conductivity.[1,2] In past decades, the discovery of fullerene, carbon nanotube, and graphene make the carbon materials one of the most promising candidates for the future electronic devices.[3–5]

Different from the huge success of carbon materials, the boron materials receive relatively less attention for the large challenge in experimental realization. Boron has three valence electrons, which makes the bonding mechanism extremely complicated, thus, the structural diversity and physical and chemical complexity are beyond those of carbon. Bulk boron is characterized by three-dimensional polyhedral structural features, in which the dominant motif is isolated B_{12} icosahedron.[6] However, the electron-deficient character of boron leads to the 2D boron structures present higher stability. Prior to the study of 2D boron sheets, the boron clusters had been found to be planar or quasi-planar,[7–9] laying the foundations for the discovery of 2D boron nanostructures. It was reported that 2D boron sheets can be constructed via removing atoms in the triangular lattice or adding atoms into the hexagonal lattice.[10] A structural parameter, named hexagonal vacancy density η, is used to describe the ratio of hexagon holes to the number of atomic sites in the original triangular lattice within one unit cell. 2D boron sheets with different η possess different electronic properties, such as high anisotropy and superconductivity.[11–13] Besides, from first-principles calculations, lots of proposed 2D boron allotropes which are not belong to the above structural paradigm have been investigated extensively with different properties.[14–19] The synthetic mechanism of 2D boron on metal substrates or metal boride substrates has been discussed with first-principles calculations,[20,21] and inspiringly, there are a few 2D boron sheets been confirmed in experiments, such as β_{12}, χ_3,[22] and δ_6.[23]

Since the successful realization of 2D boron sheets on Ag (111) substrate, 2D boron materials have attracted more and more attention.[24] For convenience, we will call the 2D boron sheet as borophene, in analogue to graphene. For better understanding of borophene, one of the most considered issues is the thermal properties of the short and strong covalent bonds in boron materials. Meanwhile, considering the bonding complexity and structural diversity, the electronic properties of borophene would be interesting. As we know, the boron atom is a light atom, and the intrinsic electron–phonon coupling is strong, therefore, the superconductivity in boron materials is also a very hot topic. Additionally, the negligible spin–orbit coupling makes the topological classifications in boron materials different from the strong spin–orbit coupling materials as discussed in carbon materials.[25,26] In this review, at first, we will introduce the notable electronic properties of borophene in Section 2, e.g., the superconductivity and topological properties. Then, we will mainly focus on the basic theories and thermal transport properties of borophene in Section 3. Although, some efforts have been dedicated to the electronic properties of borophene, researchers are mainly interested in its thermal transport. Hence, after a brief introduction of the electronic properties, we will mainly discuss the

†Corresponding author. E-mail: lidf@cqupt.edu.cn

© 2018 Chinese Physical Society and IOP Publishing Ltd

thermal transport properties of borophene. We would refer to most of the researches and achievements made in recent years and organize them in a comparative way, providing a better understanding of these materials for further studies.

1.1. Electronic properties

The nature of electron-deficient of boron atoms makes the structural complexity of its allotropes greater than that of carbon, leading to very abundant physical properties, some of them even superior to the carbon materials, such as the superconductivity and topological properties.

Compared to carbon with outer-shell valence electron $2s^2 2p^2$, boron lacks one electron with $2s^2 2p^1$. Therefore, the stable configuration of honeycomb lattice of carbon is unstable for boron. Moreover, this essential difference leads to a completely different structural landscape for boron. Because of lacking one electron, the bonding mechanism in boron sheets is usual the mixture of two-center bonding and three-center bonding. The recent experimental realization of 2D boron sheets, e.g., triangular boron, β_{12}, and χ_3, are metal. The origin of the stability and metallic properties of the boron sheet were discussed by Tang *et al.*[10] They divided the bonding state of the boron sheet into in-plane part (contributed by orbitals s, p_x, and p_y) and out-of-plane part (contributed by orbital p_z). The in-plane part forms σ bonding and anti-bonding, and the out-of-plane part forms π bonding and anti-bonding. In the normal hexagonal lattice, the three electrons do not fulfill three σ bonding states, but half-fill π bonding, which makes the hexagonal lattice of boron unstable and metallic, acting as acceptors. However, the flat triangular lattice has the Fermi level over the crossing point of σ bonding and antibonding states. The over-occupied σ antibonding states also make this sheet unstable and metallic, meanwhile, acting as donors. Ideally, the hexagon mixed with triangle with the highest stability should have electrons filling all available in-plane bonding states and the low-energy out-of-plane states, which will lead to a metallic system.

1.2. Superconductivity

According to the BCS theory, metals composed of lightweight elements are beneficial for increasing the superconducting transition temperature (T_c), because the Debye temperatures of these metals are typically high.[27] The prevailing two-dimensional materials, such as graphene, silicene, and phosphorene, are not well suited to produce high-T_c for their semimetal and semiconductor electronic properties and the weak electron–phonon coupling. However, the lighter boron materials theoretically have much stronger electron–phonon coupling; meanwhile, the metallicity of the two-dimensional boron is another critical advantage for studying the superconductivity, without needing any external charge carrier doping.

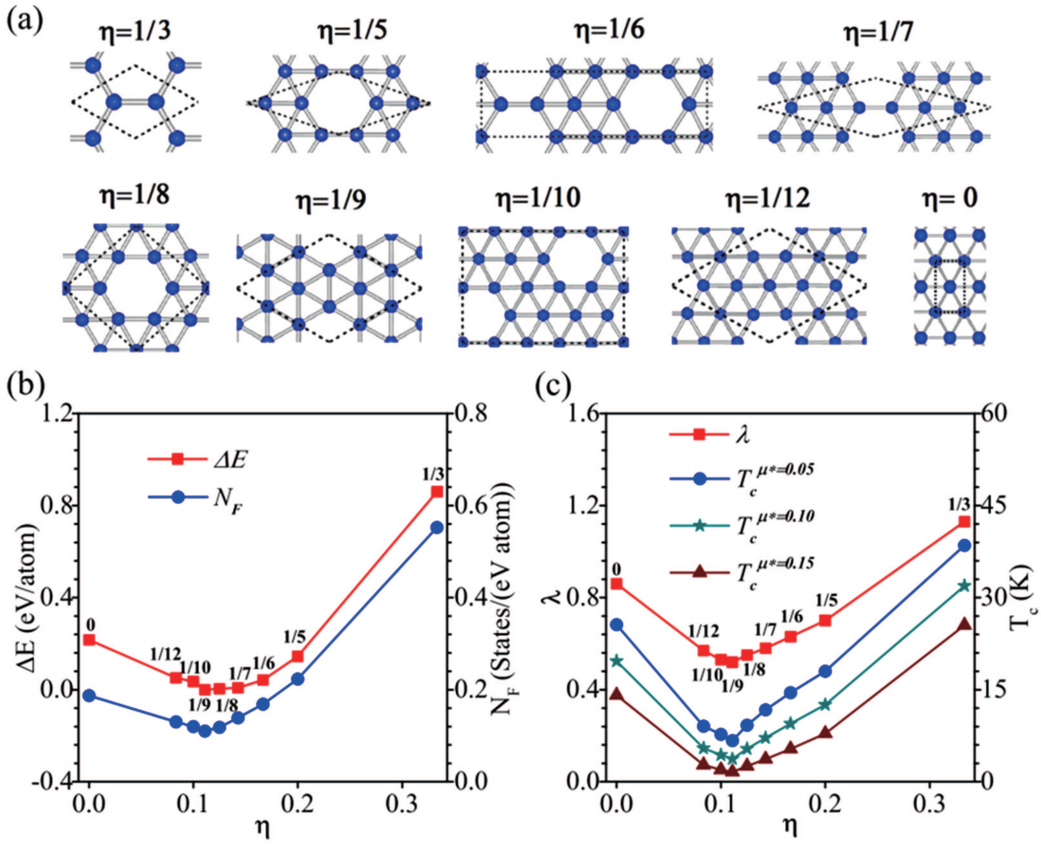


Fig. 1. (color online) (a) Most stable borophene for each given hexagon hole density η. (b) Total energy and N_F vs. η. (c) λ and T_c vs. η, with permission from Ref. [13].

The high-T_c of binary boride, such as MgB_2,[28] and the successful experimental synthesis of two-dimensional boron further impel the interest of finding the superconducting states in elemental boron materials. Considering the short history and insufficient experimental studies of two-dimensional boron allotropes for now, people study the superconductivity of boron materials mainly from the theoretical perspective.[19] Using *ab initio* evolutionary algorithm and first-principles calculations, Zhao *et al.* proposed five energetically metastable 2D boron structures, and found that the superconductivity is ubiquitous in these 2D boron materials.[29] As shown in Fig. 1, Penev *et al.*[12] and Zhao *et al.*[13] discovered the superconductivity and that T_c is a V-like function of the hexagonal hole density η in the triangular lattice. Recently, much attention was paid to the experimentally reported 2D boron structure, triangular boron, β_{12}, and χ_3. Xiao *et al.* found that the superconductivity in triangular 2D boron can be significantly enhanced by strain and carrier doping.[30] Gao *et al.* found that the electron–phonon coupling constants in the β_{12} and χ_3 are larger than that in MgB_2; and the T_c are determined to be 18.7 K and 24.7 K through the McMillian–Allen–Dynes formula,[31] which are much higher than that of graphene. Although, the experimental realization of β_{12} has been confirmed by several research groups, there is still no experimental probe about its superconductivity for now. From first-principles calculations, Cheng *et al.* argued that the expected high-T_c of β_{12} is effectively suppressed by the substrate-induced strain and electron doping, and can be enhanced by compressive strain and hole-doping.[32]

1.3. Topological properties

The discovery of graphene and the Dirac fermion feature it possessed has constantly inspired people in the last decade to search for more candidates of 2D Dirac materials.[33,34] Nowadays, 2D Dirac materials have spread to plenty materials, not bound to carbon materials only. Boron has the potential to spawn a great deal of 2D Dirac materials for its structural diversity and complexity as the left side element of carbon atom.[35]

In 2014, Zhou *et al.* proposed a 2D boron sheet named *Pmmn* boron with massless Dirac fermions using *ab initio* evolutionary structural search method, which is the first 2D Dirac boron material.[15] Due to the electron-deficient feature, boron materials could present different bonding characteristics as compared with carbon materials. For instance, Ma *et al.* reported a 2D partially ionic boron that consists of graphene-like plane and B_2 pairs that act as "anions" and "cations", respectively. In addition, this ionic structure exhibits double Dirac cones near the Fermi level with a high Fermi velocity, which is even higher than that in grapheme.[17] There are a few other works about Dirac fermions properties in 2D boron, such as a series of planar boron allotropes with honeycomb topology,[36] Dirac nodal-lines and titled semi-Dirac cones coexisting in a striped boron sheet.[37] One of the most inspiring findings of Dirac fermions in 2D boron allotropes is the successfully and firstly experimental identification of Dirac fermions in β_{12} boron sheet growth on Ag(111).[38] As presented in Fig. 2, they argued that the lattice β_{12} sheet can be decomposed into two triangular sublattices, analogues to the honeycomb lattice and, thus, host Dirac cones. Moreover, each Dirac cone can be split by introducing periodic perturbations. The current studies of topological properties have gone beyond the paradigm of Dirac fermions or Weyl fermions, been extended to multiple degenerated fermions in solid lattices, in which the Lorentz symmetry is not necessary to be respected.[39] Recently, Motohiko Ezawa presented that there could be triplet fermions in β_{12} boron sheet through altering its atomic interaction parameters and structural symmetry.[40]

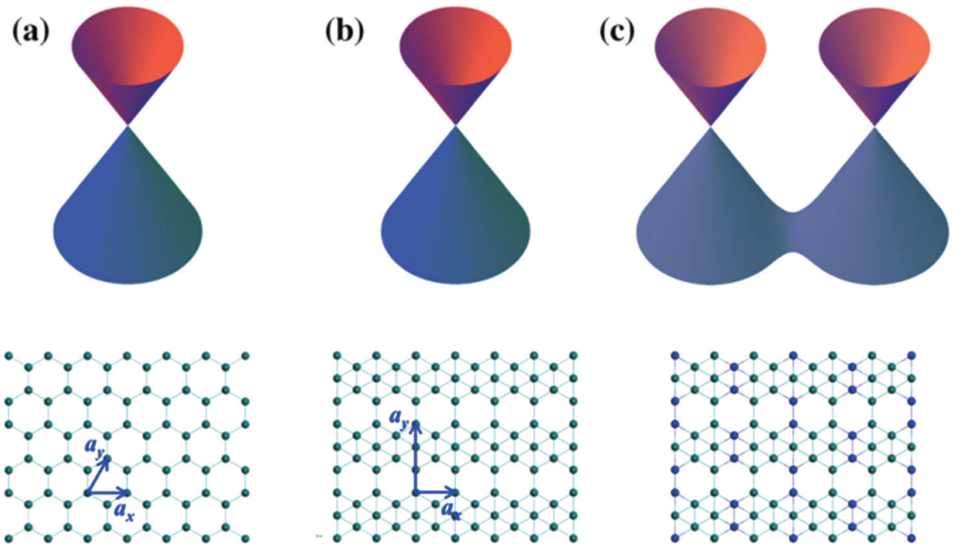


Fig. 2. (color online) The top and bottom panels are the band structures and corresponding atomic structures, respectively. (a) Honeycomb lattice. (b) β_{12} sheet. (c) The β_{12} sheet with a 3×1 perturbation, with permission from Ref. [38].

Since the boron atom is a light atom, the spin–orbit coupling (SOC) should negligible in boron materials, what makes their topological classifications quite different from those of strong spin–orbit coupling materials, as discussed in the topological properties in carbon materials.[25,26] As for superconductivity, the search for high-T_c materials has lasted for a very long time, elemental boron materials or boron compounds may be one of the greatest potential candidates for their strong electron–phonon coupling. Considering the huge interests in topological properties and superconductivity in solid state materials, we have reasonable expectation that there should be more astonishing properties waiting for discovery in boron materials.

2. Thermal transport in borophene

Since the experimental realization of the two-dimensional boron sheet (borophene), thermal transport in different phases of borophene has become an attractive topic. The highly anisotropic thermal transport and moderate thermal conductivity make borophene promising in applications of transparent conductor and thermal management. It is found that thermal transports among different phases of borophene are quite different, e.g., the thermal stability, thermal conductivity, anisotropy, etc. Different kinds of theoretical methods were adopted in the literatures, including phonon Boltzmann transport equation (pBTE), nonequilibrium Green's function (NEGF), and molecular dynamics (MD) simulations. Besides, some efforts were dedicated to the strain effect and mechanical properties of borophene. In this part, we will give a general view on the thermal transport in borophene by summarizing these achievements made in recent years, with an eye to understand the transport behavior in borophene and to call for further study on these materials.

2.1. Basic theories of thermal transport

Thermal transport is an external phenomenon of lattice vibration, specifically, characterized by the phonon transport behaviors. Macroscopically, thermal transport refers to the heat flux when a conductor is placed in a temperature gradient, while complex phonon transport and scattering mechanisms are taking place in this process microscopically. Different kinds of methods have been developed to calculate the thermal transport properties of materials, including phonon Boltzmann transport equation (pBTE), molecular dynamics (MD) simulations, and nonequilibrium Green's function (NEGF), etc. These methods show distinct features and functions. For instance, the MD simulations can simulate the thermal transport in a system with large scale and size, which simulate more like real experiment. The pBTE is a century old method based on a primitive cell and the interatomic force constants (IFCs), being more applicable and extensive. We now give a general introduction of these methods. At first, we would like to introduce pBTE since it has been developed by Wu *et al.* and widely used nowadays.[41–43] At thermal equilibrium, in the absence of external forces, the phonons are distributed according to Bose–Einstein statistics f_0. When there is a temperature gradient ∇T, phonon distribution f deviates from f_0, and this process can be described via BTE

$$\nabla T \cdot \boldsymbol{v}_\lambda \frac{\partial f_\lambda}{\partial T} + \frac{f_\lambda - f_0}{\tau_\lambda^0} = 0, \tag{1}$$

where the first term means the phonon diffusion due to ∇T, and the second term denotes the phonon scattering arising from allowed processes. The solution of this BTE is trivial because of the complex phonon scattering processes, i.e., the relaxation time τ_λ^0 cannot be accurately determined. Considering two- and three-phonon processes as the only scattering sources, Wu *et al.* defined $\boldsymbol{F}_\lambda = \tau_\lambda^0(\boldsymbol{v}_\lambda + \Delta_\lambda)$, where τ_λ^0 and $\boldsymbol{v}_\lambda$ are the relaxation time and group velocity of phonon mode λ, respectively. If Δ_λ is set to zero, the equation is equivalent to working within the relaxation time approximation (RAT). Thus, Δ_λ is the measure of the population of a specific phonon mode. τ_λ^0 and Δ_λ can be computed as

$$\begin{aligned}\Delta_\lambda &= \frac{1}{N}\sum_{\lambda'\lambda''}^{+} \Gamma^{+}_{\lambda\lambda'\lambda''}(\zeta_{\lambda\lambda''}F''_\lambda - \zeta_{\lambda\lambda'}F'_\lambda) \\ &\quad + \frac{1}{N}\sum_{\lambda'\lambda''}^{-} \frac{1}{2}\Gamma^{-}_{\lambda\lambda'\lambda''}(\zeta_{\lambda\lambda''}F''_\lambda + \zeta_{\lambda\lambda'}F'_\lambda) \\ &\quad + \frac{1}{N}\sum_{\lambda}^{'} \Gamma_{\lambda\lambda'}\zeta_{\lambda\lambda'}F'_\lambda, \end{aligned} \tag{2}$$

$$\frac{1}{\tau_\lambda^0} = \frac{1}{N}\left(\sum_{\lambda'\lambda''}^{+}\Gamma^{+}_{\lambda\lambda'\lambda''} + \sum_{\lambda'\lambda''}^{-}\frac{1}{2}\Gamma^{-}_{\lambda\lambda'\lambda''} + \sum_{\lambda}^{'}\Gamma_{\lambda\lambda'}\right), \tag{3}$$

where $\Gamma^{\pm}_{\lambda\lambda'\lambda''}$ denote the three-phonon scattering rates, i.e., the absorption and emission processes of phonons. To obtain these scattering rates, we need the scattering matrix, which depends on the anharmonic IFCs. $\Gamma_{\lambda\lambda'}$ is the scattering probabilities from isotopic disorders. The boundary scattering is not included in this method since it is a low-temperature behavior. At last, the lattice thermal conductivity κ_l can be obtained in term of $\boldsymbol{F}_\lambda$ as

$$\kappa_l^{\alpha\beta} = \frac{1}{k_B T^2 \Omega N}\sum_\lambda f_0(f_0+1)(\hbar\omega_\lambda)^2 v_\lambda^\alpha F_\lambda^\beta, \tag{4}$$

where Ω is the volume of the unit cell. This method is implemented in ShengBTE code,[43] which requires second- and third-order IFCs as input, and can simulate bulk and even low-dimensional systems.

The MD simulations usually include equilibrium MD (EMD) and nonequilibrium MD (NEMD).[44–47] The NEMD also contains two approaches, i,e., calculating heat flux by controlling the temperature gradient or conversely calculating temperature gradient by controlling the heat flux. There

are some basic concepts in MD simulations, including time step, boundary condition, statistical ensemble, empirical potential function, etc. Specifically, the NEMD simulations usually go through three steps. The first is the relaxation stage, which makes the system fully relax and reach the equilibrium state under a fixed temperature. The second is the transitional stage, transiting a period by placing the equilibrium system in a statistical ensemble. The final one is the nonequilibrium stage, turning the system from equilibrium to nonequilibrium state with a stable heat flux by applying a temperature gradient. And then, one can obtain the statistics of the heat flux and temperature distribution. The lattice thermal conductivity can be calculated according to the Fourier's law

$$\kappa_{\rm ph} = \frac{J}{A \cdot \nabla T}, \tag{5}$$

where A is the cross sectional area of the system, and ∇T is the temperature gradient. J is the heat flux, which is obtained by the slop of exchange energy $E_{\rm ex}$ to the time step

$$J = \frac{E_{\rm ex}}{A\Delta t}. \tag{6}$$

As we know, the thermal conductivity of a bulk is independent of the sample size, while it is another thing for low-dimensional systems.[48–50] Hence, calculating thermal conductivity of low-dimensional systems needs to consider different sample sizes in a large scale, and the MD simulations rightly show advantages in this kind of calculations. However, the shortage of the empirical potential function impedes a wide application of this method to various systems.

The NEGF method for phonon transport, developed by Yamamoto *et al.*, is more suitable for dealing with nanostructures.[51] This method is based on a double-electrode model. When the model is placed between the hot and cold heat baths, the thermal current can be calculated as

$$J_{\rm th} = \int_0^\infty \frac{{\rm d}\omega}{2\pi} \hbar\omega \left[f_{\rm L}(\omega) - f_{\rm R}(\omega) \right] T_{\rm ph}(\omega), \tag{7}$$

where $f_{\rm L(R)}(\omega)$ is the Bose–Einstein distribution of equilibrium phonons with energy $\hbar\omega$ in the left (right) electrode with temperature $T_{\rm L}(T_{\rm R})$, $T_{\rm ph}(\omega)$ is the phonon transport function. $T_{\rm ph}(\omega)$ can be obtained through the Green's function of the scattering region, which is calculated via the self-consistent of the Hamiltonian matrix of the model. After the Green's function of the scattering region is converged, $T_{\rm ph}(\omega)$ can be calculated as

$$T_{\rm ph}(\omega) = {\rm Tr}\left[\Gamma_{\rm L}(\omega) G_{\rm S}^{\rm r}(\omega) \Gamma_{\rm R}(\omega) G_{\rm S}^{\rm a}(\omega) \right], \tag{8}$$

where $G_{\rm S}^{\rm r/a}(\omega)$ is the retarded/advanced Green's function of the scattering region. Here, $\Gamma_{\rm L/R}(\omega) = {\rm i}\left[\Sigma_{\rm L/R}^{\rm r}(\omega) - \Sigma_{\rm L/R}^{\rm a}(\omega) \right]$, and $\Sigma_{\rm L/R}^{\rm r/a}(\omega)$ is the retarded/advanced self-energy due to the coupling to the left/right electrode. In the limit of small temperature difference between the hot and cold heat baths, the thermal conductance $\kappa_{\rm ph} \equiv J_{\rm th}/(T_{\rm L} - T_{\rm R})$ is given by[51,52]

$$\kappa_{\rm ph}(T) = \frac{\hbar^2}{2\pi k_{\rm B} T^2} \int_0^\infty {\rm d}\omega \omega^2 T_{\rm ph}(\omega) \frac{{\rm e}^{\hbar\omega/k_{\rm B}T}}{\left({\rm e}^{\hbar\omega/k_{\rm B}T} - 1 \right)^2}. \tag{9}$$

2.2. Thermal stability and conductivity of borophene

Among all different types of boron sheets predicted theoretically,[19] the phases of β_{12}, χ_3, and δ_6 have been experimentally reported in recent years, all grown epitaxially on Ag(111) substrate and showing weak interaction with the substrate.[22,23] However, these boron sheets may not be thermally stable after leaving the substrate, especially for the δ_6 phase. In spite of this reality, people have taken much effort to investigate the thermal transport in δ_6 phase borophene. We summarized the main results in Table 1. The δ_6 phase borophene has two atoms per unit cell with the space group *Pmmn*, along armchair direction are parallel linear chains while a remarkable buckling is observed along the zigzag direction, indicating a high anisotropy. The experimental lattice constants are $a = 5$ Å and $b = 2.89$ Å.[22] As compared to experimental borophene with the substrate, it can be found in Table 1 that the optimized parameter of free-standing borophene is almost unchanged along the zigzag (b-axis) direction while only about 1/3 to the experiment along the armchair direction (a-axis).

The phonon spectra of borophene (δ_6) obtained by finite displacement (FDS) method and density function perturbation theory (DFPT) are shown in Fig. 3.[53,54] The two boron atoms in the unit cell form six dispersion branches, including three acoustic and three optical branches, the same as graphene, silicene, phosphorene, etc.[55] In Fig. 3, both FDS and DFPT point to an imaginary frequency of ZA branch along the Γ–X (armchair) direction, which indicates the instability of the long-wavelength transverse thermal vibrations. This phenomenon in turn may explain the stripe formation along the armchair direction in the synthesis of borophene.[54] In contrast to the previous two-dimensional materials, the phonon dispersion of borophene shows a highly anisotropy along armchair (Γ–X) and zigzag (Γ–Y) directions. Importantly, the optical branches along Γ–X are more dispersive than that along Γ–Y, indicating the high optical phonon velocities along the armchair direction, which would remarkably contribute to the thermal conductivity. Besides, Sun *et al.* pointed out the stronger B–B bonding along armchair direction by analyzing the polarized vibrations.[54] All these characteristics are associated with the thermal transport behaviors.

In order to deal with the instability of δ_6 borophene, i.e., the imaginary frequency near Γ point, two efficient empirical potentials for MD simulations were developed to describe the interaction of borophene with low energy triangular structure by Zhou *et al.*[57] One is the linear potential valence force

filed (VFF) mode, and the other is the nonlinear Stillinger-Weber (SW) potential. The VFF mode is useful for the description of interatomic interactions in covalent materials, in which the interactions are associated with some bond stretching and angle bending components. The SW potential is one of the most efficient nonlinear potentials, which includes both linear and nonlinear interactions. The linear component of the SW potential can be derived based on the VFF mode. As shown in Fig. 3(c), the imaginary frequency near Γ point disappears since the long-range interaction is not considered in these modes and potentials. Their MD simulations were performed within the publicly available package LAMMPS. Another strategy of removing the instability is full hydrogenation, and the hydrogenated product is now called borophane. After the full hydrogenation, there are two boron atoms and two hydrogen atoms in the unit cell, with an increased lattice constant a and an almost unchanged lattice constant b (Table 1), as compared to borophene.[58] The increased lattice constant a corresponds to the significantly stretched B_1–B_1 bond, which is 1.613 Å in borophene while 1.935 Å in borophane.[58] From Fig. 3(d), one can notice that all the phonon frequencies are positive in the whole Brillouin zone, showing that the hydrogenated borophene (borophane) is dynamically stable. Thus, the hydrogenation can effectively improve the stability of borophene. It is interesting that the hydrogen atoms dominate the high frequency branch and show weak interaction with lower phonon branches due to its light atomic mass.

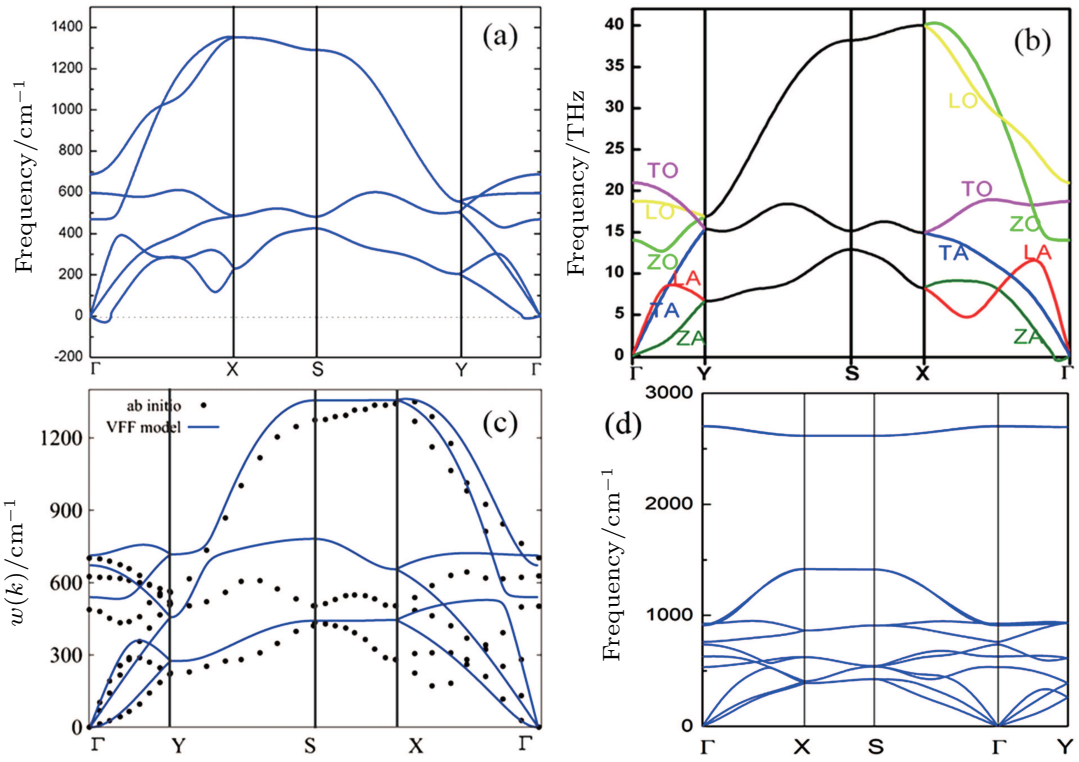


Fig. 3. (color online) Phonon spectra of δ_6 borophene calculated by (a) density function perturbation theory (DFPT) and (b) finite displacement (FDS) method, adapted with permission form Refs. [53] and [54], respectively. (c) Phonon spectrum calculated by molecular dynamics simulations within valence force filed (VFF) mode, compared to the result of *ab-initio* calculation, with permission from Ref. [57]. (d) The phonon spectrum of fully hydrogenated borophene (borophane), adapted from Ref. [58].

In addition to the δ_6 phase borophene, people also concentrated on the thermodynamic properties of other phases of borophene, i.e., the β_{12}, χ_3, α, and $\alpha\prime$ phases.[56,59,60] To our surprise, these phases seem more stable than δ_6 since their phonon spectra have no imaginary frequency. According to the different symmetry of the geometric structure, their transport behaviors are also different. For example, the α and $\alpha\prime$ phases are isotropic with a symmetrical phonon dispersion, while the anisotropy of δ_6, β_{12}, and χ_3 phases is observed through the difference in the phonon dispersion around Γ between [Γ–X] and [Γ–Y]. As can be found in the previous calculations, the allowed phonon frequencies for different phases of borophene are quite similar since the components are the same B atoms. However, different number of B atoms per unit cell result in different number of optical phonon branches, along with the distinct geometric symmetry, leading to multiple thermal transport in these borophene.[19,59] Thermal conductivity is a direct index to describe the phonon transport properties, which provides some guidance for possible applications of the materials. For instance, a high thermal conductivity is necessary to removing the accumulated heat in electronic or photovoltaic devices, while a low thermal conductivity is pursued by thermoelectric and thermal insulation community.

We also collected the available thermal conductivity of borophene at room temperature calculated by different kinds of methods, as shown in Table 1. It is found that the ther-

mal conductivity of borophene is much lower than that of graphene. The thermal conductivity of δ_6 borophene at room temperature is 43.3×10^{-9} W/K and 22.6×10^{-9} W/K along armchair and zigzag directions,[54] respectively, calculated through pBTE, which are quite lower than 1775×10^{-9} W/K of graphene.[61] The low thermal conductivity of borophene arises mainly from the small extension of acoustic dispersion with the low group velocities. One notices that the thermal conductivity along zigzag direction is about half of that along armchair direction, the higher value in armchair direction can be attributed to the stronger B–B bonding and the highly dispersive optical branches along this direction.[54] Zhou *et al.*[56] calculated the thermal conductance of borophene by ballistic NEGF method. They calculated the ballistic phonon transport and found superior lattice thermal conductance of borophene, which helps to understand the size effect and transport behavior in borophene. In contrast to borophene, borophane possesses a higher thermal conductivity along zigzag direction, which means that the full hydrogenation of borophene changes the anisotropy of the thermal transport. This unusual phenomenon is confirmed by group velocity and scattering mechanism, as presented by Liu *et al.*[58] It can also be found in Table 1 that the thermal conductivities calculated by different methods are quite similar, e.g., the results of δ_6 obtained by pBTE and MD are very close to each other.[54,62] We also find that the $\alpha\prime$ borophene has an isotropic and low thermal conductivity of 5.96×10^{-9} W/K,[60] which behaves more like monolayer TMDCs, e.g., monolayer ZrS_2, HfS_2, etc.[63,64] The low thermal conductivity of α' compared to δ_6 is due to a large number of optical branches and also the strong coupling of acoustic and optical branches with high scattering rates. The diversity of thermal transport in different borophene makes it possible in applications of transparent conductor and thermal management.

Table 1. The lattice parameters, room temperature thermal conductivity, thermal stability, and computational method of borophene from related literatures. Some thermal conductivities in corresponding literature are unavailable. Not that the unit of thermal conductivity is normalized in 2D form.

Phase		a/Å	b/Å	$\kappa_1\ (a,b)/10^{-9}$ W/K	Thermal stability	Method
		5[22]	2.89(exp.)			
		1.613[53]	2.864		No	
		1.617[54]	2.872	(43.3, 22.6)	No	pBTE
δ_6		1.612[56]	2.869		No	NEGF
		2.1[62]	3.18	(42.6, 22.01)	No	MD
	(VFF/SW)	1.614[57]	2.866		Yes	MD
	(hydrogen)	1.93[58]	2.82	(79.7, 147.8)	Yes	pBTE
α'		4.37[60]	4.37	5.96	Yes	pBTE
β_{12}		5.062[56]	2.924		Yes	NEGF
8-*Pmmn*		4.52[65]	3.25	(61.9, 86.1)	Yes	pBTE

From discussions above, we know that thermal transport in different borophene exhibits special properties. Specifically, some are highly anisotropic while other are isotropic; some are intrinsically stable while some are thermally unstable; the magnitude of thermal conductivity shows much difference owing to the different phonon scattering rates. It is noticed that studies on the thermal transport of borophene are still lacking since the thermal conductivities of some phases of borophene are unknown, which call for further studies. We now take a look at the size dependency of the thermal conductivity. The phonon mean free paths of δ_6 borophene, calculated via pBTE, are 300 nm and 400 nm for the armchair and zigzag directions, respectively,[54] which are six orders of magnitude smaller than those of graphene. The short mean free path of borophene also points to its lower thermal conductivity. In MD simulations, the calculated thermal conductivity usually shows a strong size dependency until the sample length is smaller than the allowed phonon mean free path.[62] The thermal conductivity by MD increases with increasing sample length, and the converged thermal conductivity is close to that by pBTE. At last, it is worthwhile to note that 8-*Pmmn* borophene was taken as an example to confirm the intrinsic quadratic acoustic branch of 2D systems and also its effect on thermal conductivity.[65] Using physical IFCs, they showed that a quadratic dispersion phonon branch is always presented on suspended few-layer systems, which can have a strong impact on the thermal conductivity of 2D systems. The physical IFCs result in a negligible change of the phonon dispersion, except for turning the lowest acoustic mode to a quadratic dispersion near Γ, which has a dramatic effect on the thermal conductivity, decreasing by 50%. Hence, the quadratic dispersion of the lowest phonon branch is a universal feature of 2D systems.

2.3. Strain effect on borophene

The instability of borophene (δ_6) made people try to study its mechanical properties by applying tensile strains. Both Pang and Wang have calculated the strain effect on the mechanical flexibility and phonon instability.[66,67] Their results are much similar, both indicated that the mechanical properties along armchair and zigzag directions are highly anisotropic. As shown in Table 2, when applying uniaxial strains, the critical strains along armchair and zigzag directions are 0.08 and 0.15, respectively, showing the superior flexibility along

zigzag direction, which corresponds to the higher flattened strain (by 27%) of the bucking height along this direction. As for the biaxial strain, the critical strain is 0.08.[67] For both uniaxial strain along armchair and biaxial strain, the phonon spectra are dynamically unstable when the bond lengths are extended by 8%, suggesting a lower limit for which the structure remains stable along the out-of-plane direction. In contrast, such phonon mode remains stable under uniaxial strain along zigzag direction. No matter what kind and how strong the strain is applied, the imaginary frequency cannot be fully removed, which indicates that the freestanding borophene is mechanically unstable even with strains, and the stability of the synthesized borophene is probably provided by the out-of-plane constraints from the silver substrates.

In Table 2, borophene can withstand stress up to 20.26 N/m and 12.98 N/m in armchair and zigzag directions, respectively. The phonon calculations indicate that under uniaxial tension along the zigzag direction, the failure is attributed to the elastic instability, whereas along armchair direction and biaxial tension, the failure mechanism is phonon instability and such instability is dictated by the out-of-plane acoustic mode.[67] The critical strengths of borophene are obviously higher than those of silicene and black phosphorus,[68,69] while much smaller than that of graphene,[70] which is because the B–B bonds are stronger than the Si–Si and P–P bonds, while weaker than the C–C bonds in graphene. It is found that the critical strain of borophene may be the lowest among all the studied 2D materials. The failure mechanisms of silicene and graphene are similar, that is the elastic instability under both uniaxial and biaxial tensions. While the failure mechanisms of borophene are found to be similar to MoS_2,[71] with one of the elastic instability while the rest two of the phonon instability. What is more, the critical strengths and strains of borophene are more anisotropic than those of silicene and graphene because of their hexagonal structures.

As we know, borophene can be stabilized by hydrogenation. Wang *et al.* have calculated the mechanical properties and phonon stability of strained borophane.[72] They considered uniaxial tensile strains along armchair and zigzag directions, and also the biaxial strains. The critical strains are 0.12, 0.3, and 0.25 for uniaxial strain along armchair and zigzag directions, and biaxial strain, respectively, see Table 2. Thus, the mechanical properties of borophane are also highly anisotropic, and the armchair direction also possesses the superior mechanical flexibility. The calculated phonon dispersions under different strains indicate that borophane can withstand up to 5%, 15% uniaxial tensile strains along armchair and zigzag directions, respectively, and 9% biaxial strains, which means that borophane may become unstable before reaching the critical strains.[72] As one notices, the strain that borophane can withstand along the zigzag direction is three times of that along the armchair direction. Consequently, borophane exhibits better mechanical stability and phonon stability along the zigzag direction.

Table 2. Lattice parameters, critical tensile strain, and corresponding ultimate strength for different borophene. The strains applied include uniaxial strain along armchair direction, uniaxial strain along zigzag direction, and the biaxial strain.

	a/Å	*b*/Å	Buckling height/Å	Uniaxial (armchair)	Uniaxial (zigzag)	Biaxial
					Critical tensile strain	
					Ultimate strength/N·m^{-1}	
δ_6	1.614[67]	2.866	0.911	0.08	0.15	0.08
				20.26	12.98	14.75
Borophane	1.941[72]	2.815	0.81	0.12	0.3	0.25
				12.26	18.48	21.06
β_{12}	5.062[74]	2.924	0	0.2	0.21	
				19.97	20.38	
χ_3	2.9[74]	4.44	0	0.21	0.155	
				19.91	20.18	
α	5.046[74]	5.044	0.17	0.21	0.16	
				14.84	18.83	

Recently, Mortazavi *et al.* studied the strain effect on the thermal conductivity of borophene by MD simulations.[62] The calculated thermal conductivities at room temperature are 42.63×10^{-9} W/K and 22.01×10^{-9} W/K for armchair and zigzag directions, respectively, being consistent with the results of pBTE (Table 1). As for the strain effect, they observed that there is a significantly increase in thermal conductivity along armchair direction when the strain is applied in this direction, while there is just a smaller increase for zigzag direction.[62] However, they did not analyze in depth why it behaves like this. This different response is associated with the anisotropic crystal of borophene, which reinforces the prospective application in the construction of phononic device. It is worthwhile to note that borophene may not be suitable for thermoelectric applications since it has a metallic behavior and the thermal conductivity does not reach the required lower limit.

In Table 2, we also show the stain effect and mechanical properties of other borophene phases, i.e. β_{12}, χ_3, and α.[73,74] Along armchair direction, their critical tensile strains are higher than that of δ_6, indicating a better flexibility of these sheets along armchair direction. This also points to

the possible phonon instability of δ_6 along armchair direction against long-wavelength transversal waves, and these borophene phases are more stable than δ_6 borophene. While along zigzag direction, they critical strains are close to δ_6 but still a little higher, with the higher ultimate tensile strengths along this direction. In contrast to δ_6, for which the zigzag direction has superior flexibility, these boron sheets have better flexibility along armchair direction especially for χ_3 and α sheets. This difference is attributed to the different atomic configurations and the way they evolve and rearrange during the loading condition.[74] Along armchair direction, the ultimate strengths of β_{12} and χ_3 are very close to each other, of which the fully occupied hexagonal or zigzag lattices are connected by single B–B bonds. When stretched along zigzag direction, the fully occupied hexagonal lattices in β_{12} can extend more than zigzag lattices in χ_3 borophene.[74] These results can help to understand the stability and mechanical properties of borophenes.

2.4. Borophene nanoribbon

The discovery of borophene also draws immediate attention to the investigation of borophene nanoribbons (NRs). The magnetism, electronic and phonon transport properties of borophene NRs were predicted by first-principles calculations. It was found that pristine δ_6 armchair NRs are non-magnetic, while zigzag NRs adopt magnetic ground states, either anti-ferromagnetic or ferromagnetic depending on the ribbon width.[75] Upon hydrogenation, all turn to non-magnetic. Liu *et al.* discovered negative differential resistance and magnetoresistance in zigzag borophene NRs.[76] Hence, borophene NRs can be built with different structures and magnetic moment. These electronic properties can be taken into account in the design of devices involving these NRs.

Recently, several kinds of borophene NRs were synthesized on Ag (100) surface, which may promote further applications of borophene.[77] Jia *et al.* have studied the thermal transport in borophene (δ_6) NR by MD simulations.[78] The length of the sample they chosen for simulation is 40 nm, while the width varies from 10 nm to 30 nm. The thermal conductivity of zigzag NRs is much higher than that of armchair NRs, i.e., 586.12 W/mK and 257.62 W/mK, respectively. It was found that the thermal conductivity of the NRs shows weak dependence on the widths, and also shows little sensitivity to the strains. The thermal conductivity does not change as the strain increases from 0.5% to 2%, applying along the heat flux direction. Zhang *et al.* also studied the phonon transport in borophene NRs with other phases, i.e., β_{12} and χ_3, both exhibiting diverse phonon transport abilities and different anisotropies.[79] They mainly compared the transport properties with that of graphene, among theses NRs the highest thermal conductance is comparable to that of graphene, whereas the lowest thermal conductance is less than half of graphene. Overall, the experimental synthesis and the novel thermal properties of borophene NRs enrich the low-dimensional allotrope of boron and possible applications in thermal management devices.

As a closing of this part, we try to highlight the special thermal transport in different phases of borophene. A general view of the thermodynamic, mechanical properties and even the borophene nanoribbons is given, which may provide a reference for further studies on the thermal transport of borophene. However, to our knowledge, the instability of borophene is still not fully understood, and also the anisotropic response of the thermal transport to the strain effect is not clear. What is more, the achievements made in recent years are mainly based on the striped δ_6 borophene, thermal transport in some of the boron sheets is still unknown. These questions call for continuous study on the thermal transport and mechanical properties of borophene.

3. Conclusion

As we can see from this review, the investigation of borophene is growing explosively. At first, we mainly focus on the crucial electronic properties of borophene, i.e., the superconductivity and topological properties. The strong electron–phonon coupling and metallic nature of borophene make it promising candidate of superconductivity. Meanwhile, borophene is also observed as a two-dimensional Dirac material with high Fermi velocity. Following the electronic properties, we also review the thermal transport properties of borophene. A comparison of the thermal transport and mechanism properties of different borophene has been made, displaying the potential application of borophene on transparent conductor and thermal management. Borophene exhibits various investigations and applications of certain community. In this work, we merely give a general view on the thermal and electronic properties, which point to its promising applications in thermal conductor, nanoelectronic devices, etc. However, most of these achievements were made theoretically through first-principles calculations. Further experiments should focus more on these novel physical properties.

References

[1] Castro Neto A H, Peres N M R, Novoselov K S and Geim A K 2009 *Rev. Mod. Phys.* **81** 109
[2] Geim A K and Novoselov K S 2007 *Nat. Mater.* **6** 183
[3] Hirsch A 2010 *Nat. Mater.* **9** 868
[4] Singh V, Joung D, Zhai L, Das S, Khondaker S I and Seal S 2011 *Prog. Mater. Sci.* **56** 1178
[5] Dresselhaus MS 2012 *Phys. Scr.* **T146** 014002
[6] Albert B and Hillebrecht H 2009 *Angew. Chem. Int. Ed. Engl.* **48** 8640
[7] Sai L, Wu X, Gao N, Zhao J and King R B 2017 *Nanoscale* **9** 13905
[8] Zhao J, Huang X, Shi R, Liu H, Su Y and King R B 2015 *Nanoscale* **7** 15086
[9] Piazza Z A, Hu H S, Li W L, Zhao Y F, Li J and Wang L S 2014 *Nat. Commun.* **5** 3113
[10] Tang H and Ismail-Beigi S 2007 *Phys. Rev. Lett.* **99** 115501
[11] Li X B, Xie S Y, Zheng H, Tian W Q and Sun H B 2015 *Nanoscale* **7** 18863

[12] Penev E S, Kutana A and Yakobson B I 2016 *Nano. Lett.* **16** 2522
[13] Zhao Y, Zeng S and Ni J 2016 *Appl. Phys. Lett.* **108** 242601
[14] Penev E S, Bhowmick S, Sadrzadeh A and Yakobson B I 2012 *Nano. Lett.* **12** 2441
[15] Zhou X F, Dong X, Oganov A R, Zhu Q, Tian Y and Wang H T 2014 *Phys. Rev. Lett.* **112** 085502
[16] Zhang Z, Yang Y, Gao G and Yakobson B I 2015 *Angew. Chem. Int. Ed. Engl.* **54** 13022
[17] Ma F, Jiao Y, Gao G, Gu Y, Bilic A, Chen Z and Du A 2016 *Nano Lett.* **16** 3022
[18] Gao N, Wu X, Jiang X, Bai Y and Zhao J 2017 *FlatChem*
[19] Wu X, Dai J, Zhao Y, Zhuo Z, Yang J and Zeng X C 2012 *ACS Nano* **6** 7443
[20] Liu H, Gao J and Zhao J 2013 *Sci. Rep.* **3** 3238
[21] Liu Y, Penev E S, Yakobson B I 2013 *Angew. Chem. Int. Ed. Engl.* **52** 3156
[22] Mannix A J, Zhou X F, Kiraly B, Wood J D, Alducin D, Myers B D, Liu X, Fisher B L, Santiago U and Guest J R 2015 *Science* **350** 1513
[23] Feng B, Zhang J, Zhong Q, Li W, Li S, Li H, Cheng P, Meng S, Chen L and Wu K 2016 *Nat. Chem.* **8** 563
[24] Zhang Z, Penev E S and Yakobson B I 2016 *Nat. Chem.* **8** 525
[25] Zhong C, Chen Y, Yu Z M, Xie Y, Wang H, Yang S A and Zhang S 2017 *Nat. Commun.* **8** 15641
[26] Zhong C, Chen Y, Xie Y, Yang S A, Cohen M L and Zhang S B 2016 *Nanoscale* **8** 7232
[27] Bardeen J, Cooper L N and Schrieffer J R 1957 *Phys. Rev.* **108** 1175
[28] An J M and Pickett W E 2001 *Phys. Rev. Lett.* **86** 4366
[29] Zhao Y, Zeng S and Ni J 2016 *Phys. Rev. B* **93** 014502
[30] Xiao R C, Shao D F, Lu W J, Lv H Y, Li J Y and Sun Y P 2016 *Appl. Phys. Lett.* **109** 122604
[31] Gao M, Li Q Z, Yan X W and Wang J 2017 *Phys. Rev. B* **95** 024505
[32] Cheng C, Sun J T, Liu H, Fu H X, Zhang J, Chen X R and Meng S 2017 *2D Mater.* **4** 025032
[33] Wehling T O, Black-Schaffer A M and Balatsky A V 2014 *Adv. Phys.* **63** 1
[34] Wang J, Deng S, Liu Z and Liu Z 2015 *Natl. Sci. Rev.* **2** 22
[35] Zhou X F and Wang H T 2016 *Adv. Phys: X* **1** 412
[36] Yi W C, Liu W, Botana J, Zhao L, Liu Z, Liu J Y and Miao M S 2017 *J. Phys. Chem. Lett.* **8** 2647
[37] Zhang H, Xie Y, Zhang Z, Zhong C, Li Y, Chen Z and Chen Y 2017 *J. Phys. Chem. Lett.* **8** 1707
[38] Feng B, Sugino O, Liu R Y, Zhang J, Yukawa R, Kawamura M, Iimori T, Kim H, Hasegawa Y and Li H 2017 *Phys. Rev. Lett.* **118** 096401
[39] Bradlyn B, Cano J, Wang Z, Vergniory M G, Felser C, Cava R J and Bernevig B A 2016 *Science* **353** aaf5037
[40] Ezawa M 2017 *Phys. Rev. B* **96** 035425
[41] Li W, Mingo N, Lindsay L, Broido D A, Stewart D A and Katcho N A 2012 *Phys. Rev. B* **85** 195436
[42] Li W, Lindsay L, Broido D A, Stewart D A and Mingo N 2012 *Phys. Rev. B* **86** 174307
[43] Li W, Carrete J, Katcho N A and Mingo N 2014 *Comp. Phys. Comm.* **185** 1747
[44] Müller-plathe F 1999 *Phys. Rev. E* **59** 4894
[45] Griebel M, Knapek S and Zumbusch G 2007 Berlin: Springer
[46] Nose S 1984 *J. Chem. Phys.* **81** 511
[47] Tan X J 2013 *Theoretical Study on the Thermoelectric Properties of Carbon Nanotubes and Related One-dimensional structures* (Ph. D Dissertation) (Wuhan: Wuhan Univertity)
[48] Sellan D P, Landry E S, Turney J E, McGaughey A J H and Amon C H 2010 *Phys. Rev. B* **81** 214305
[49] Li W, Carrete J and Mingo N 2013 *Appl. Phys. Lett.* **103** 253103
[50] Gu X and Yang R 2014 *Appl. Phys. Lett.* **105** 131903
[51] Yamamoto T and Watanabe K 2006 *Phys. Rev. Lett.* **96** 255503
[52] Markussen T, Jauho A P and Brandbyge M 2009 *Phys. Rev. Lett.* **103** 055502
[53] Peng B, Zhang H, Shao H, Xu Y, Zhang R and Zhu H 2016 *J. Mater. Chem. C* **4** 3592
[54] Sun H, Li Q and Wan X G 2016 *Phys. Chem. Chem. Phys.* **18** 14927
[55] Ge X J, Yao K L and Lü J T 2016 *Phys. Rev. B* **94** 165433
[56] Zhou H, Cai Y, Zhang G and Zhang Y W 2017 *2D Mater. Appl.* **1** 14
[57] Zhou Y P and Jiang J W 2017 *Sci. Rep.* **7** 45516
[58] Liu G, Wang H, Gao Y, Zhou J and Wang H 2017 *Phys. Chem. Chem. Phys.* **19** 2843
[59] Tsafack T and Yakobson B I 2016 *Phys. Rev. B* **93** 165434
[60] Xiao H, Cao W, Ouyang T, Guo S, He C and Zhong J 2017 *Sci. Rep.* **7** 45986
[61] Balandin A A, Ghosh S, Bao W, Calizo I, Teweldebrhan D, Miao F and Lau C N 2008 *Nano Lett.* **8** 902
[62] Mortazavi B, Le M Q, Rabczuk T and Pereira L F C 2017 *Physica E* **93** 202
[63] Lv H Y, Lu W J, Shao D F, Lu H Y and Sun Y P 2016 *J. Mater. Chem. C* **4** 4538
[64] Lv H Y, Lu W J, Luo X, Lu H Y, Zhu X B and Sun Y P 2016 arXiv: 1608.05464
[65] Carrete J, Li W, Lindsay L, Broido D A, Gallego L J and Mingo N 2016 *Mater. Res. Lett.* **4** 204
[66] Pang Z, Qian X, Yang R and Wei Y 2016 arXiv:1602.05370
[67] Wang H, Li Q, Gao Y, Miao F, Zhou X F and Wan X G 2016 *New. J. Phys.* **18** 073016
[68] Yang C, Yu Z, Lu P, Liu Y, Ye H and Gao T 2014 *Comput. Mater. Sci.* **95** 420
[69] Wei Q and Peng X 2014 *Appl. Phys. Lett.* **104** 251915
[70] Liu F, Ming P and Li J 2007 *Phys. Rev. B* **76** 064120
[71] Li T 2014 *Phys. Rev. B.* **90** 167402
[72] Wang Z, Lü T Y, Wang H Q, Feng Y P and Zheng J C 2016 *Phys. Chem. Chem. Phys.* **18** 31424
[73] Peng B, Zhang H, Shao H, Ning Z, Xu Y, Ni G, Lu H, Zhang D W and Zhu H 2017 *Mater. Res. Lett.* **5** 399
[74] Mortazavi B, Rahaman O, Dianat A and Rabczuk T 2016 *Phys. Chem. Chem. Phys.* **18** 27405
[75] Meng F, Chen X, Sun S and He J 2017 *Physica E* **91** 106
[76] Liu J, Chen C, Han L, Zhu Z and Wu J 2017 arXiv:1701.08501
[77] Zhong Q, Kong L, Gou J, Li W, Sheng S, Yang S, Cheng P, Li H, Wu K and Chen L 2017 *Phys. Rev. Mater.* **1** 021001
[78] Jia Y, Li C, Jiang J W, Wei N, Chen Y and Zhang Y J 2017 arXiv:1705.11016
[79] Zhang Z, Xie Y, Peng Q and Chen Y 2016 *Nanotechnology* **27** 445703